ANALYSIS OF THE XENON FEEDBACK ON THE CORE DYNAMICS OF HIGH-TEMPERATURE REACTORS DURING HEAT REMOVAL TRANSIENTS WITHOUT REACTOR SHUTDOWN

RAHIM NABBI *Kernforschungsanlage Jülich*
Institut für Nukleare Sicherheitsforschung, Postfach 1913, D-5170 Jülich 1
Federal Republic of Germany

Received June 3, 1983
Accepted for Publication August 23, 1983

The core dynamic analysis of an anticipated heat removal transient without scram in a high-temperature gas-cooled reactor has indicated that in case of a failure of core cooling, the reactor undergoes a self-shutdown after 1 min because of its negative temperature coefficients of reactivity. If the decay heat removal system operates according to plant specification, recriticality, and thus nuclear power generation, occurs. However, the maximum rise in fuel elements temperature is limited to 50°C due to the high heat capacity of the core.

Without taking into consideration the effect of xenon feedback on the neutron kinetics, a new steady core state is established after 2 h in which the fuel temperature and gas outlet temperature at the lower core edge are 195°C higher than in normal operation. Due to transient xenon poisoning, a rise in gas outlet temperature only occurs during the first 70 min and amounts to 70°C. For this reason undesirable transient strains on the components connected behind the core are not expected. A slow xenon buildup during the first hour ensures a long-term subcriticality of the reactor. Without any contribution from the shutdown system, this leads to a decrease in nuclear power and thus to core cooling with functioning decay heat removal.

INTRODUCTION

In the case of accidents in high-temperature reactors with spherical fuel elements, the power generation must be reduced rapidly enough to the decay heat level. This generally takes place by means of the reactor scram system, which is initiated via the limit criteria for the facility's various safety variables. The scram system, including its excitation signals, is designed in such a way that the probability of its failure on request remains extremely small. Nevertheless, a failure cannot be completely excluded.

There is a series of transients that require a reactor scram as a result of disturbances in the operational heat removal system.[1,2] An example of this is failure of the blowers in the main coolant system, in the course of which an automatic safety procedure for decay heat removal is started by initiating the reactor scram system.[3]

If one presumes that the reactor shutdown does not come into action for a fairly long period of time in the case of failure of the main cooling system, anticipated transient without scram, but that the decay heat removal system comes into operation, then recriticality can be expected as a result of core cooling.[2,4,5] The associated concomitant increase in power generation or fuel element temperatures is primarily determined by the temporal course of heat removal. In addition, the transient behavior of the xenon poisoning is significant for the core dynamics because of the temperature dependency of the xenon absorption cross section and the change in its concentration.

The influence of xenon feedback on the core dynamics is being investigated in this paper with the aim of determining the consequences of failure of the reactor shutdown systems during heat removal transients of the type described and of possibly deriving special requirements for the shutdown devices. The analyses were carried out for the example of a pebble bed high-temperature gas-cooled reactor (HTGR) with a thermal power of 500 MW. Because of the different system specifications, the applicability of the results to the other HTGRs is limited to a certain degree.

DESCRIPTION OF THE CORE STRUCTURE

A pebble bed HTGR with a thermal power of 500 MW was designed for the generation of nuclear process heat in the "Prototype Plant Nuclear Process Heat Project (PNP)" (Fig. 1, Ref. 3). The 6-cm-diam spherical fuel elements generate a mean power density of 4 MW/m^3. The fuel element spheres consist of a 5-cm-diam graphite matrix in which the fuel particles coated with graphite shells are embedded.

In the two-region core, the degree of enrichment amounts to 6.1 and 15% ^{235}U (low enriched uranium). On average, the fuel element spheres are removed from the reactor after 4 yr corresponding to the once through then out (OTTO) loading cycle, in which fresh fuel spheres are continuously fed in at the top and spent spheres discharged at the bottom.[6] The most important design data for this HTGR plant are shown in Table I.

The helium coolant flows through the core from top to bottom at 40 bar and is heated from 303 to 990°C. The decay heat is removed by a separate heat removal system that consists of four independent, noninteracting helium-helium heat exchanger loops with associated back cooling loops.

The shutdown system in the PNP-500 consists of two independent shutdown devices. The first shutdown system is provided in the form of 36 separate absorber rods having a reactivity worth of $10.0. In the case of the reactor scram, they are activated by interruption of the current to trip magnet coil and will freely fall to their end position in the boreholes of the side reflector. The second system consists of 54 absorber rods that are designed to be pneumatically driven into the pebble bed used for reactor control and shutdown. The reactor scram is achieved by partial insertion of these core rods to 100 cm and by activation of all reflector rods. The reactivity absorption amounts to about $18.0 and is sufficient for a rapid scram from any operating condition. For reactor shutdown over a long time range, additional reactivity resulting from cooling down of the core and decay of the ^{135}Xe has to be compensated. This will be achieved by driving the core rods deeper into the core with the additional reactivity of $25.7.

TABLE I

Nuclear Design Data of the Pebble Bed HTGR (PNP-500)

Core	
Height/radius, cm	507.5/280
Total power (thermal), MW	500
Average power density, MW/m^3	4.0
Helium inlet/outlet temperature, °C	303/990
Helium mass flow, kg/s	139
Reflector thickness	
Top/bottom/side, cm	200/100/130
Enrichment zones	
Number	2
Outer radii, cm	196/280
Fuel sphere	
Total radius, cm	3.0
Radius of the fuel matrix, cm	2.5
Fuel material	UO_2
Heavy-metal content per sphere, g	8
Coated fuel particle	
Density of kernels, g/cm^3	10.9
Thickness of coatings, μm	90/40/35/35
Density of coatings, g/cm^3	0.9/1.85/3.2/1.85
Average burnup, MWd/ton	100.000
^{235}U enrichment, inner/outer, %	6.8/12.6

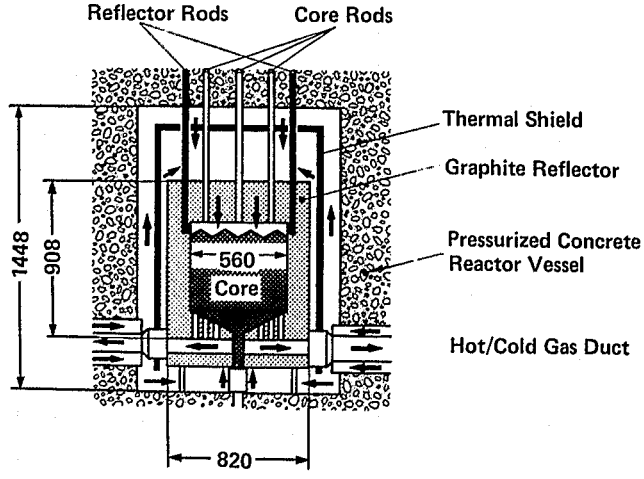

Fig. 1. Schematic of the pebble bed high-temperature reactor PNP-500 with coolant flow directions (dimensions are in centimetres).

REPRESENTATION OF THE ANTICIPATED TRANSIENT

The anticipated heat removal transient begins with a faulty initiation of the signal to turn off the blowers at all the steam generator blower units. All blowers thus come to a stop, whereby the coolant gas flow drops very rapidly. The reactor scram is initiated if the response threshold for the diverse system variables is reached. These are mainly the gas flow rate, the ratio of the neutron flux to the mass flow, or rotational speed of the blowers.

The mass flow returns to zero after 120 s corresponding to the blower coasting curve typical of HTGRs. It is assumed that the reactor shutdown system does not go into action on request by the protective devices but that the decay heat removal loops are put into operation according to plant specifications after 4.5 min.

If all the decay heat removal loops are started up simultaneously on request, then up to four times as much heat as necessary can be removed. This leads to an undesirably rapid core cooling. In order to avoid this, an automatic operational "summation control" of all the decay heat loops is provided that limits the total heat removal to the cooling capacity of a single loop.[3]

Helium flow rates are assumed for the analyses carried out here which correspond to the single or double blower delivery of the decay heat removal loops. It was assumed that the gas mass flow would rise from 0 to 6 or 12 kg/s within 30 s with utilization of the decay heat removal system after the blowers had come to a stop. The temporal course of the helium flow up to 6 min after the beginning of the transient is shown in Fig. 2.

MODEL OF THE REACTOR CORE

The analysis described here was carried out with the reactor kinetics code SHOVAV-Jül (Ref. 7). This program is a spatially one-dimensional space/time kinetics code that is based on a multigroup diffusion approximation for neutron transport. Up to four energy groups as well as six groups of delayed neutrons can be incorporated into the calculations.

The material composition of the reactor core is modeled by subdividing the core into a certain number of horizontal segments. To each segment a set of cross sections is assigned that corresponds to the local mixture of nuclides.

The present results were obtained with a division into 11 segments, the first and last segment representing the top and bottom reflectors, respectively (as fuel-free zones). Subdivision of the active core into 9 segments proves to be sufficiently good to model the axial fuel distribution, which has a distinct power maximum in the upper part of the reactor core (Fig. 3). This distribution is conditioned by the predefined procedure for loading the core fuel.

All the neutron cross sections can be treated as temperature-dependent values in order to determine the temperature dependency of the reactivity. This is achieved by providing a set of cross sections for each segment in the reactor core for various temperatures which are then used as supporting points for a polygonal approximation of the cross sections as a function of temperature. The current cross sections are calculated by the program from the present moderator and fuel temperature during the course of a transient.

These temperatures are calculated in a subroutine on the basis of a thermohydraulic model of the reactor core that is coupled with the neutronics section in such a way that the neutron kinetics equations and the thermohydraulic equations form a system of partial differential equations that is simultaneously solved by means of numerical methods.[7]

The energy equation for the reactor core consists of two coupled differential equations. These are the gas convection equation for the gas flow through the pebble bed and the thermal conduction equation for heat transport within the fuel spheres. The two differential equations are coupled via heat transfer coefficients for which empirical correlations are used.[8] Temporal transients in this system are significantly determined by the large heat capacity of the fuel spheres.

The geometric grid for the solution of thermofluid dynamic equations is the same as that of the material segments of the reactor core already mentioned. The temperature distribution in the fuel

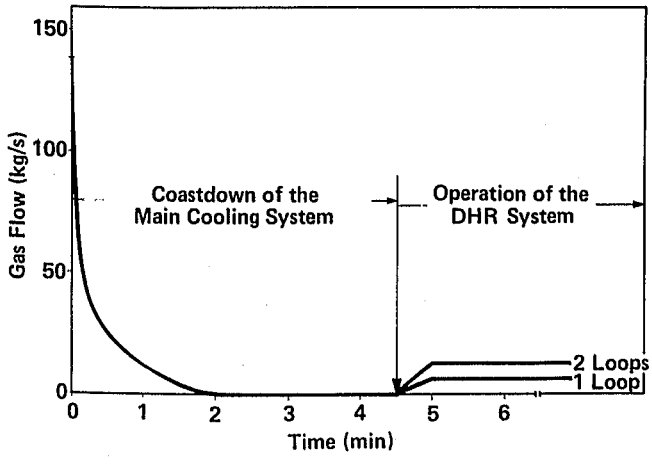

Fig. 2. Mass flow rate during the blower coastdown and after the start of the DHR system.

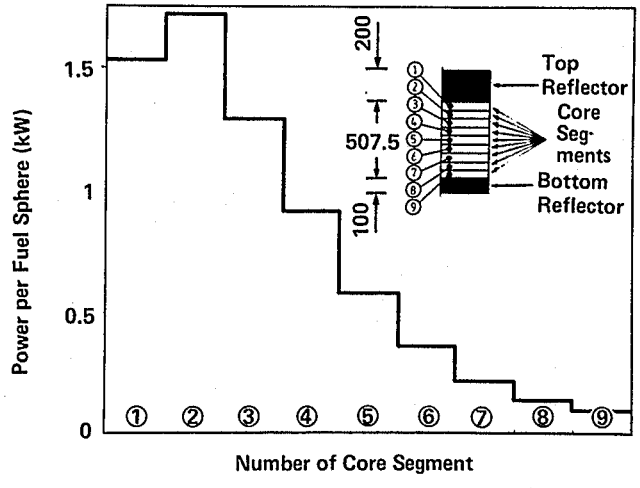

Fig. 3. Axial distribution of the fuel sphere power with a geometric core mode (dimensions are in centimetres).

spheres is calculated in each segment for a "representative" sphere. The inner region of the fuel spheres, which consists of coated fuel particles embedded in a graphite matrix, is treated as though it were homogeneous. The resulting mean temperature of the representative sphere is interpreted as the moderator temperature. The mean temperature of the fuel kernel of the coated particles is used as the fuel temperature. This temperature is generally higher than the moderator temperature due to the heat transfer resistance of the particle coating.

The difference between the fuel temperature and moderator temperature is determined from the solution of the thermal conduction equation for a representative fuel particle in each fuel sphere.[7]

The influence of the transient xenon poisoning on the reactivity absorption is included in SHOVAV-Jül on the basis of a feedback model. In this the concentrations of the isotopes ^{135}I and ^{135}Xe are calculated as time dependent, i.e., as the solutions to the system of differential equations that describe the buildup and decay of these isotopes as a function of the thermal neutron flux. In calculating the reactivity absorption by xenon, the temperature dependence of the absorption cross section of ^{135}Xe is taken into consideration. The time dependence of the reactivity absorption by ^{135}Xe is calculated separately for each of the axial core segments corresponding to the local thermal neutron flux.

GENERATION OF THE FEW-GROUP CROSS SECTIONS

The macroscopic four-group cross sections of the core segments were generated for the one-dimensional core dynamic calculations. To this end, zero-dimensional spectral calculations were carried out for various moderator and fuel temperature supporting points using the MUPO computer code.[9] Thereby the group constants of the MUPO nuclear data library were condensed from 43 to 4 energy groups. The structure of these neutron energy groups is compiled in Table II. The nuclide compositions for these calculations were generated from the two-dimensional nuclide density arrays in the design calculations[10] and volume averaged in a radial direction. The group-dependent buckling values were used in order to take into consideration the neutron leakages during the zero-dimensional spectral calculations. The procedure for generation group data for the kinetic calculation is represented in Fig. 4.

Similarly, the 43 group constants of the MUPO data library for ^{135}Xe were also condensed to 4 energy groups with the local neutron spectrum. The absorption cross section of the fourth energy group together with the space-dependent xenon concentration in question was used to take into account the contribution of the xenon absorption. The energy dependence of the absorption cross section of ^{135}Xe from the MUPO data library is shown in Fig. 5.

TABLE II

Boundaries of the Neutron Energy (eV)

Group 1	Group 2	Group 3	Group 4
1.00E+08[a] 748.5	17.6	1.90	0.0025

[a]Read as 1.00×10^8.

The effective six-group data of the delayed neutrons were used for the transient calculations, these being determined for each core segment corresponding to the precursor concentration on the basis of conservation of the total number of delayed neutrons. The effective group-dependent decay constants as well as the fraction of delayed neutrons are represented in Table III as a function of the core segment.

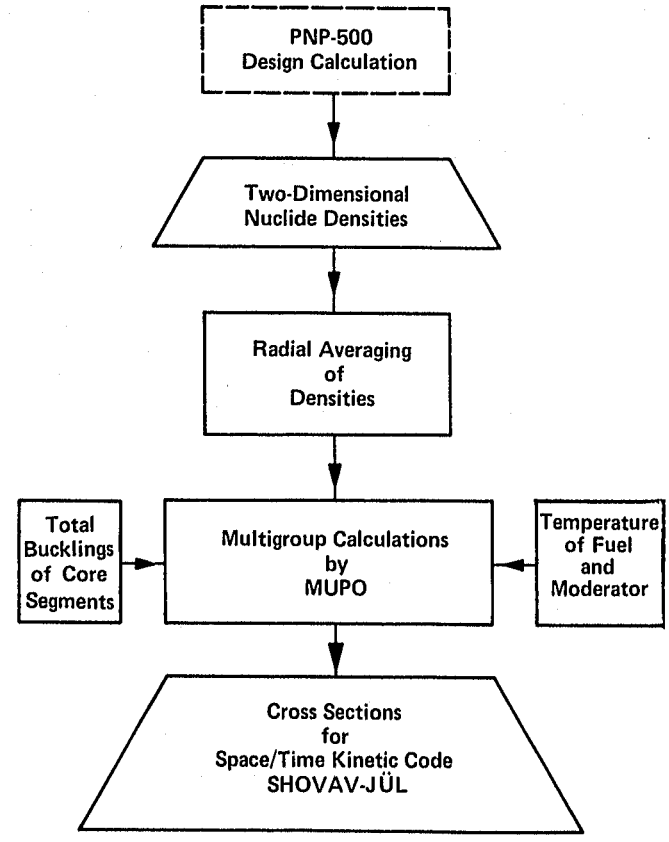

Fig. 4. A flow chart of the few-group data generation for the reactor kinetic calculations.

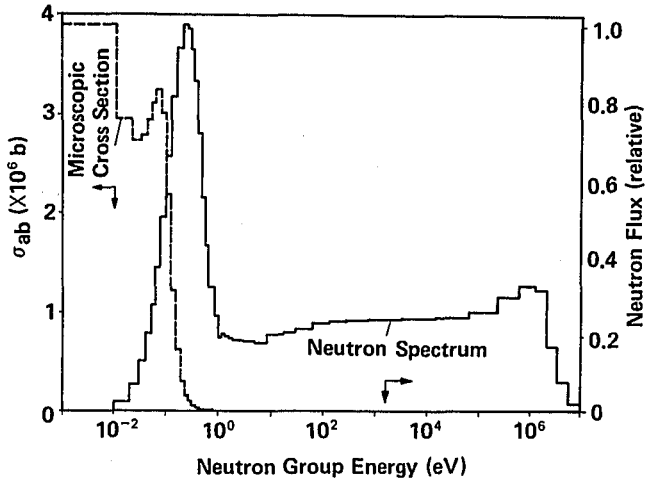

Fig. 5. Neutron spectrum at the upper part of the core and the absorption cross section of ^{135}Xe as a function of neutron energy.

RESULTS OF THE ANALYSIS AND DISCUSSION

The results of investigations on the transient behavior of the core for the anticipated operational transient in the heat removal system are depicted in Figs. 2 and 6 through 13. The calculations are based on the temporal courses of the coolant flow rate according to Fig. 2. The results of the computer simulation taking the xenon feedback into consideration are represented by the solid graphs. In comparison, the broken graphs represent those results that are obtained for the constant equilibrium concentration of ^{135}Xe.

Figure 6 shows the temporal course of the total reactivity and the reactor power during the first hour after the anticipated transient with a final flow rate of 6 kg/s, which corresponds to the power of a decay heat removal (DHR) loop. The fuel element temperatures rise when the blowers begin to coast down, followed by a decrease in core cooling. They are depicted in Fig. 7 for various core depth positions on the core axis.

As a result of the initial core heatup within the

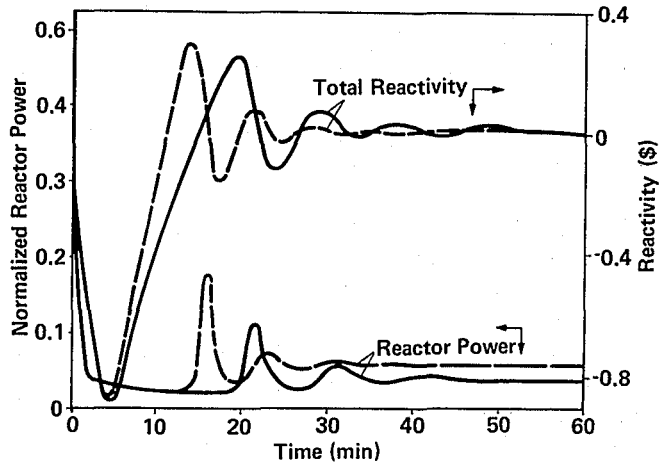

Fig. 6. Temporal course of the reactivity and power during the anticipated transient (with and without the xenon feedback).

TABLE III

Calculated Group- and Region-Dependent Delayed Neutron Fractions with Effective Decay Constants

Effective Delayed Neutron Fractions (%)							
Regions	Groups						Sum
	1	2	3	4	5	6	
1	0.020	0.135	0.118	0.235	0.068	0.025	0.601
2	0.017	0.120	0.103	0.200	0.060	0.021	0.521
3	0.014	0.112	0.093	0.182	0.057	0.018	0.477
4	0.013	0.108	0.089	0.173	0.055	0.017	0.455
5	0.012	0.106	0.086	0.168	0.055	0.016	0.444
6	0.012	0.105	0.085	0.165	0.054	0.016	0.437
7	0.012	0.104	0.084	0.163	0.054	0.015	0.433
8	0.012	0.104	0.083	0.162	0.054	0.015	0.431
9	0.012	0.104	0.083	0.162	0.054	0.015	0.431
Effective Decay Constants (s^{-1})							
---	0.0125	0.0302	0.117	0.322	1.33	3.01	---

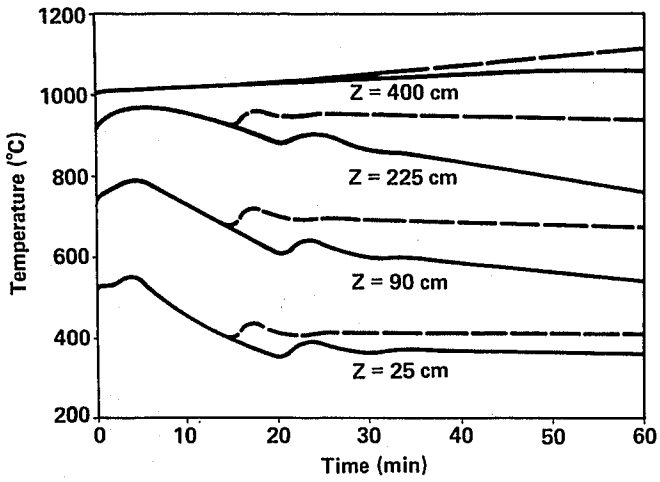

Fig. 7. Transients of the average temperature of the fuel spheres at different core depths.

first 60 s, the reactor is automatically shut down by the negative temperature coefficient of reactivity and becomes subcritical to such a degree that the heat removal briefly exceeds the reactor power due to the instantaneous mass flow. This leads to a slight decrease in fuel element temperatures in the upper core region. Due to the lack of reactor cooling in the period up to 270 s, the core temperatures rise once again, whereby the reactivity decreases further to a minimum. In this time range, the reactor power is determined by the decay heat production.

After passing through a minimum, the reactivity increases with the beginning of core cooling by the DHR system. According to Fig. 6, the reactor becomes critical again after 16 min in the case of time-dependent poisoning by ^{135}Xe. In its further course, the rise in reactor power also leads to a rise in fuel element temperatures after passing through a minimum. This brings about a limitation of the reactivity to a maximum and a subsequent decrease. In the subsequent period, this process is repeated several times with decreasing amplitude and results in a similar course for the reactor power. In comparison to this, the computer results indicate that the fuel element temperatures in the lowest core region rise continuously up to t = 45 min after the beginning of the transient.

In this region of the core, the temporal course of the fuel element temperatures is not only determined by the ratio of the sphere power to coolant flow but also by the local gas temperature. As a result of the rising gas temperatures, the heat flux from the fuel element sphere is reduced and leads to a slight increase in temperature.

Results of comparative calculations with a xenon concentration kept constant indicate that the recriticality point is delayed by 5.5 min by the buildup of xenon. As can be seen from Fig. 6, the rise in reactor power and fuel element temperatures occurs with a delay of 6.0 min. The difference in power maximum thus amounts to 6.4% of full power.

A new steady core state is established in the longer time range by neglecting the xenon buildup. In this state, the fuel element temperatures at the lower edge of the core are 195°C higher than in normal operation. In contrast to this, the computer results show that as a result of transient xenon poisoning, the reactor will remain slightly subcritical in the long term so that the reactor power, and thus the fuel element temperatures, will decrease. In the course of this, the reactivity absorption as a result of the xenon buildup is compensated with some delay through the negative temperature coefficient of reactivity. This delay is conditioned by the thermal capacity of the core.

Figure 8 represents the axial distribution of the maximum fuel temperature 2 h after the beginning of the transient. This is the fuel temperature in the center of the fuel element sphere as a function of core depth. The steady-state distribution of the central sphere temperatures in full power operation is also shown in this figure by way of comparison.

As a result of the considerable decrease in power in the upper core region, the maximum fuel temperatures are reduced there. Taking xenon feedback into consideration, this leads to a temperature difference of 350°C at a core depth of 1.80 m. Without any influence from transient xenon poisoning, we are dealing with a new steady-state distribution of the maximum fuel temperature in the core.

The temporal course of the gas outlet temperature up to 2 h after the beginning of the anticipated heat removal transient is shown in Fig. 9. As a result

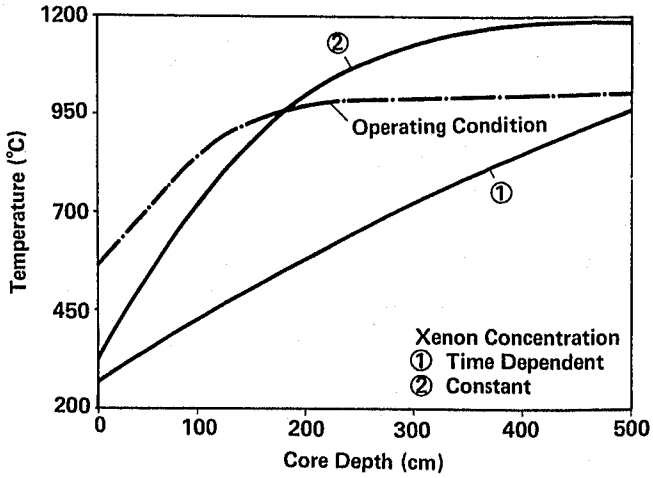

Fig. 8. Axial distribution of the temperature of the fuel kernels in the center of the spheres 2 h after the beginning of the anticipated transient (with ① and without ② the xenon feedback).

of transient xenon poisoning, it only rises to a maximum of 1060°C, and in its further course is reduced due to decreasing power generation. Undesirable strains on the components connected behind the core are thus not to be expected in the case of the transient analyzed without a contribution from the shutdown systems. A new steady core state with a gas outlet temperature increased by 195°C is then established without taking xenon feedback into consideration.

The results of calculations for the heat removal transient with a blower power of two DHR loops of 12 kg/s are shown in Figs. 10 through 13. It can be seen from the reactivity and power course in Fig. 10 that, as a result of the more rapid core cooling due to the higher mass flow, the reactor becomes critical after 8 min, i.e., 8 min earlier than in the previous case with time-dependent xenon poisoning. The reactor power increases corresponding to the relatively rapid increase in reactivity due to the temperature decrease. As in the previous case, this leads to a temperature increase (Fig. 11) and thus to a reduction in reactivity, due to which the reactor power decreases after passing through a maximum of 30% of the initial value. In the further course, the total power is determined by the mass flow and amounts to ~12% of the initial value.

The axial distribution of the central sphere temperature 2 h after the beginning of the transient together with that for the state of equilibrium is depicted in Fig. 12. By way of comparison, this figure contains the corresponding temperature distribution for the heat removal transient with the final flow of 6 kg/s. The difference in the axial distribution at t = 2 h is to be found in the different level and in the temporal course of the reactor power as a result of the different core cooling.

To demonstrate the influence of the core cooling procedure on the temporal course of the gas outlet temperature, the results of the calculations are shown in Fig. 13. In the case of a mass flow of 12 kg/s, the gas outlet temperature first rises up to a maximum of 1080°C and, in comparison with the one-loop case (6 kg/s), pursues a relatively rapid drop in the following time. The outlet temperature at t = 2 h after the beginning of the anticipated transient amounts to 845°C and is 120°C lower than that of the one-loop case. Compared with the plant operating value of 990°C, this means a temperature decrease of 145 and 25°C, respectively.

Because of the different transient behavior of the ^{135}Xe after many hours, the long-term dynamics of the core will be different from that discussed above.

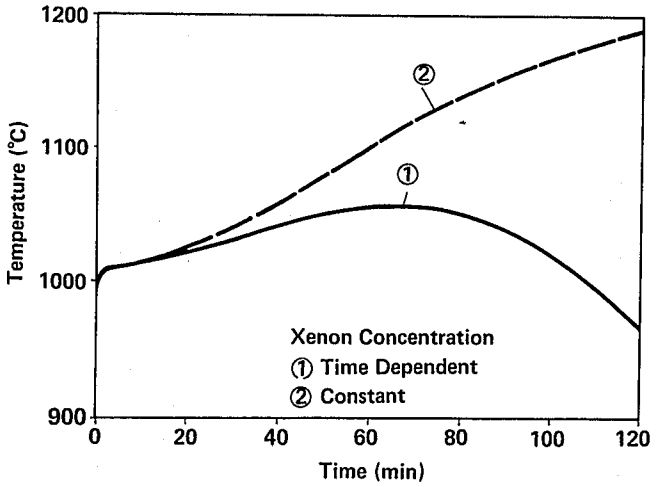

Fig. 9. Temporal course of the gas outlet temperature 2 h after the beginning of the transient (with ① and without ② the xenon feedback).

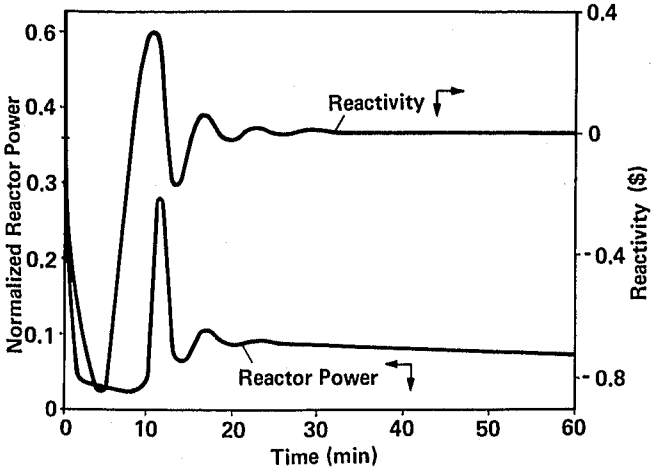

Fig. 10. Temporal course of the reactivity and power during the anticipated transient with the double loop heat removal capacity (12 kg/s).

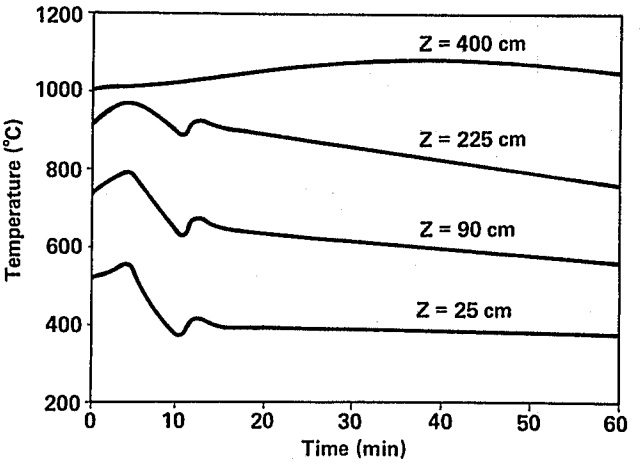

Fig. 11. Temporal course of the average temperature of the fuel spheres during the anticipated transient with the double loop heat removal capacity (12 kg/s).

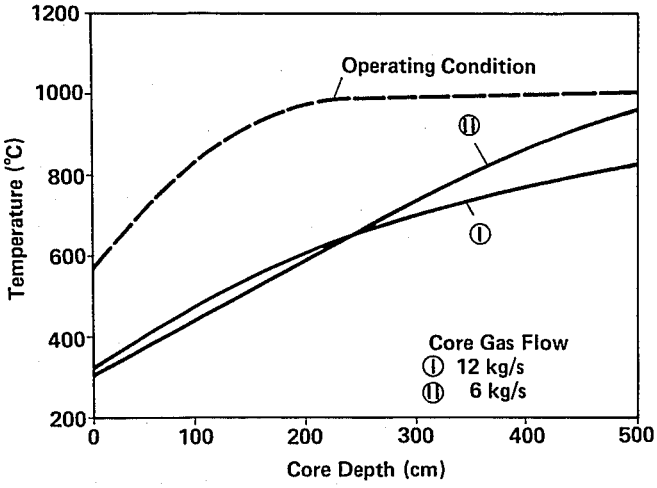

Fig. 12. Axial distribution of the temperature of the fuel kernels in the center of the fuel spheres 2 h after the beginning of the transient for two different mass flow rates.

The atomic density of xenon decreases as a result of the decay process after passing through a maximum by 9 h, which leads to a slight reactivity, power, and temperature increase. The reactivity growth following the xenon decay will be compensated for by the negative temperature coefficients with some delay. The rate of the temperature increase would be small because of the high heat capacity of the HTGR core and comparable with the rate of temperature decrease presented in this paper. The dynamics of the HTGR core under these conditions at the beginning of the anticipated transient has been investigated and reported in Ref. 11. The time range of many hours is, however, sufficiently great to activate the diverse protective devices limiting the power generation and temperature transient.

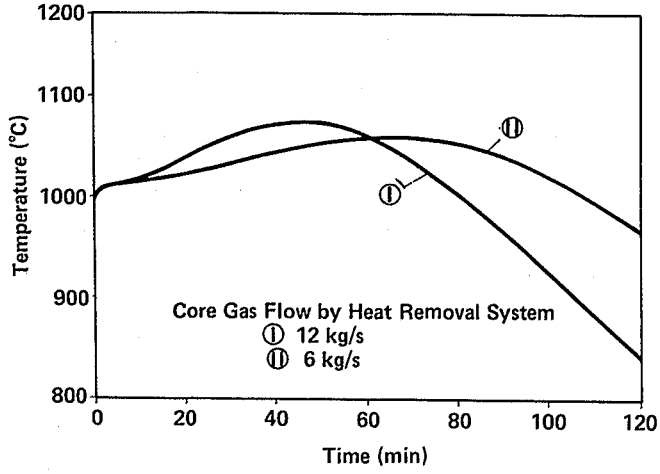

Fig. 13. Temporal course of the gas outlet temperature 2 h after the beginning of the anticipated transient for two different mass flow rates.

CONCLUSION

In the case of transients with failure of the main cooling system in a pebble bed HTGR, the reactor power generation is reduced as quickly as possible to the decay heat level by means of the reactor scram system. A relatively rapid cooling of the reactor core results with the removal of this heat by the DHR system.

For the anticipated failure of the main cooling system and without any protective actions by the control and shutdown rods, the results of the computer simulation indicate that the reactor experiences a self-shutdown after 1 min. This is a result of the inherent reactivity feedback mechanisms leading to a negative reactivity conditioned by the initial core heatup, which is limited to a temperature rise of 50°C. In this time range, the reactor scram is initiated and the DHR system is activated by the plant protection system if the safety response threshold for certain system variables, such as gas flow rate, ratio of the neutron flux to the mass flow, or rotational speed of the blowers, is exceeded.

The response of the core to the anticipated transients in the following period of time is determined by the DHR procedures resulting in criticality, assuming the failure of the shutdown systems. Nuclear power is generated at a level according to the coolant mass flow after passing a maximum. The temperature increase following the power rise remains below 50°C because of the high heat capacity of the HTGR core.

The transient behavior of the core within the ensuing hours is influenced by the time-dependent xenon poisoning. This effects a gradual decrease in reactor power and fuel temperature. The decrease of the gas outlet temperature and fuel temperature at the bottom region of the core result, however, after 1 h through passing a maximum of 1060°C. This means that the failure of the shutdown-related control systems is not associated with any undesirable strain on the core and components connected behind it. For this reason, conditioned by the slight subcriticality of the system, there are no particular demands to be made on the promptness of the shutdown systems in order to limit the consequences of this type of transients. In a longer time range, however, the functional capability of the shutdown systems should be assured in order to safely limit power generation and temperature transient.

ACKNOWLEDGMENTS

The author is indebted to J. Fassbender, head of the Institute for Nuclear Safety Research at the KFA-Jülich for his encouragement, and to G. Meister and J. Wolters for the fruitful discussions. He wishes to express his gratitude to the members of the theoretical section of the Institute for Reactor Development of the KFA-Jülich for the design data of the prototype pebble bed HTGR PNP-500.

REFERENCES

1. W. ULLRICH and W. FRISCH, "Investigations of Anticipated Transients Without Reactor Scram and Other Selected Safety Devices," *Nucl. Technol.*, **41**, 185 (1978).

2. H.-D. HECKHOFF, "Untersuchung von Betriebsstörungen ohne Reaktorschnellabschaltung (ATWS) beim Hochtemperaturreaktor," Jül-1743, Kernforschungsanlage Jülich (Oct. 1981).

3. Berbau-Forschung GmbH, GHT Gesellschaft für Hochtemperaturtechnik mbH, Hochtemperatur-Reaktorbau GmbH, Kernforschungsanlage Jülich GmbH, Rheinische Braunkohlenwerke AG, "Referenzkonzept der Prototypanlage Nukleare Prozeßwärme PNP: Gesamtanlage und Kraftwerk" (Feb 1981).

4. R. NABBI and G. MEISTER, "Einfluß der Xenon-Dynamik bei HTR auf den Ablauf von Wärmeabfuhrstörfällen mit Versagen des Abschaltsystems," *Jahrestagung Kerntechnik*, Mannheim (May 1982)

5. H. ENGELBRECHT, "Analysen zur Dynamik von Kugelhaufen-Hochtemperaturreaktoren," Jül-Spez-123, Kernforschungsanlage Jülich (Aug. 1981).

6. U. HANSEN, R. SCHULTEN, and E. TEUCHERT, "Physical Properties of the 'Once Through Then Out' Pebble-Bed Reactor," *Nucl. Sci. Eng.*, **47**, 132 (1972).

7. R. NABBI, G. MEISTER, R. FINKEN, and M. HABEN, "SHOVAV-JÜL: Ein eindimensionales Neutronenkinetik-Programm für Kugelhaufen-Hochtemperaturreaktoren mit Temperatur- und Xenon-Rückkopplung," Jül-Spez-171, Kernforschungsanlage Jülich (Sep. 1982).

8. Verein Deutscher Ingenieure, "VDI-Wärmeatlas, Berechnungsblätter für den Wärmeübergang," Verlag des Vereins Deutscher Ingenieure, Düsseldorf (1977).

9. J. SCHLÖSSER, "MUPO, An IBM-7090 Programme to Calculate Neutron Spectra and Multi Group Constants," Dragon Report 172, Atomic Energy Establishment, Winfrith (1963).

10. E. TEUCHERT, U. HANSEN, and K. A. HAAS, "V.S.O.P.—Computer Code System for Reactor Physics and Fuel Cycle Simulation," Jül-1649, Kernforschungsanlage Jülich (Mar. 1980).

11. G. MEISTER and R. NABBI, "Coredynamische Untersuchungen von Wärmeabfuhrstörfällen bei HTR unter ungünstigen Anfangsbedingungen," *Jahrestagung Kerntechnik*, Berlin (June 1983).